

Article

Water–Gas Shift Activity of Pt Catalysts Prepared by Different Methods

Hilde Bjørkan ^{1,2}, Magnus Rønning ¹ , Hilde J. Venvik ¹, Tue Johannessen ^{3,†} and Anders Holmen ^{1,*}

¹ Department of Chemical Engineering, Norwegian University of Science & Technology (NTNU), N-7491 Trondheim, Norway; Hilde.Bjorkan@sintef.no (H.B.); magnus.ronning@ntnu.no (M.R.); Hilde.j.Venvik@ntnu.no (H.J.V.)

² SINTEF Industry, N-7465 Trondheim, Norway

³ Department of Chemical Engineering, Technical University of Denmark (DTU), DK-2800 Lyngby, Denmark; Tue.Johannessen@maersk.com

* Correspondence: anders.holmen@ntnu.no

† Current Address: A.P Møller – Maersk A/S, 1263 Copenhagen K, Denmark.

Received: 31 August 2020; Accepted: 25 September 2020; Published: 1 October 2020

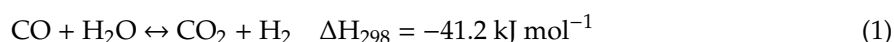


Abstract: Platinum supported on ceria and zirconia was prepared through different preparation methods: Coprecipitation (CP), spray drying (SD), and flame spray pyrolysis (FSP). The catalysts were characterized by XRD, TPR, N₂ adsorption, and H₂ chemisorption, and the water–gas shift activity in the range 190–310 °C and initial stability at 300–310 °C were tested. Although the spray-dried Pt/CeO₂/ZrO₂ catalyst shows the highest initial activity, it deactivates rapidly at 300 °C and levels out at similar activity as the coprecipitated Pt/CeO₂ and Pt/CeO₂/ZrO₂ within a few hours. Flame spray pyrolysis appears to be a promising preparation method concerning the stability of catalysts, although the initial activity is rather poor. High activity is related to high Pt dispersion, low reduction temperature, and small support particles. The support particle size is also much affected by the preparation method.

Keywords: water–gas shift; Pt catalyst; preparation; spray drying; flame spray pyrolysis

1. Introduction

The water–gas shift (WGS) reaction has been an important step in industrial hydrogen production from hydrocarbons since the early 1940s:



Recently, there is a renewed interest in the reaction because of its importance in the production of hydrogen feed with a low CO level for fuel cell applications [1]. New technologies require improved catalysts, since the commercial Cu/ZnO/Al₂O₃ catalyst has limitations that will cause problems. One disadvantage is that this catalyst is designed to operate at steady-state conditions for a long time without interruption, whereas the catalysts for fuel processing have to deal with many start-up/shutdown cycles. In addition, operation at too high temperatures must be avoided, since the sintering of copper in these catalysts starts at about 330 °C [2]. It is also sensitive to oxygen and poisoned by sulfur [3]. The use of precious metals has been widely investigated. Precious metal catalysts are stable at higher temperatures; they are nonpyrophoric and also more tolerant of catalyst poisons such as sulfur. A recent review focuses on the use of Pt-based catalysts for WGS [4]. Ceria provides interesting support for precious metals, which are not easily oxidized by water and thus have, in general, poor WGS activity. By using ceria as support, CO adsorbed on the metal can react with oxygen from ceria [5].

Ceria based catalysts are, however, prone to deactivation under reaction conditions [6,7], and hence promoters and stabilizers are used to improve the performance of the catalyst. The application of cerium–zirconium mixed oxides has become quite prominent, and the incorporation of zirconium into the ceria fluorite-type structure is expected to improve the activity and stability of the mixed oxide [1,8–10]. The preparation method highly influences the properties of the ceria supported catalysts as well [11–14]. Flame spray pyrolysis and spray drying are methods that are expected to give high surface area catalysts with finely dispersed active metal. The short residence time at high-temperature results in the formation of small particles, and the homogeneous precursor solution yields homogeneous precipitate particles [15–20]. Such properties are considered beneficial for the water–gas shift reaction [12,21–25].

In this study, Pt catalysts supported on ceria and/or zirconia were synthesized by three different preparation methods: Coprecipitation/impregnation, spray drying, and flame spray pyrolysis. The effect of the preparation methods on the characteristics and WGS activity for the catalysts was investigated.

2. Results and Discussion

2.1. Characterization

Figure 1 shows the XRD patterns of the catalysts. Crystalline CeO_2 and ZrO_2 supports are detectable for most of the catalysts. An exception is $\text{Pt}/\text{ZrO}_2\text{-SD}$, where ZrO_2 seems to be crystalline when it is prepared by coprecipitation or flame spray pyrolysis, but extremely broad peaks are observed when it is prepared by spray drying. Despite a calcination temperature of $650\text{ }^\circ\text{C}$, zirconia seems to have an amorphous structure in $\text{Pt}/\text{ZrO}_2\text{-SD}$. Due to the low Brunauer–Emmet–Teller (BET) surface area, it is not very probable that it consists of very small particles. The ceria particle sizes are very close to those of the coprecipitated samples, indicating that also the spray-dried samples are more agglomerated than the samples prepared by flame spray pyrolysis.

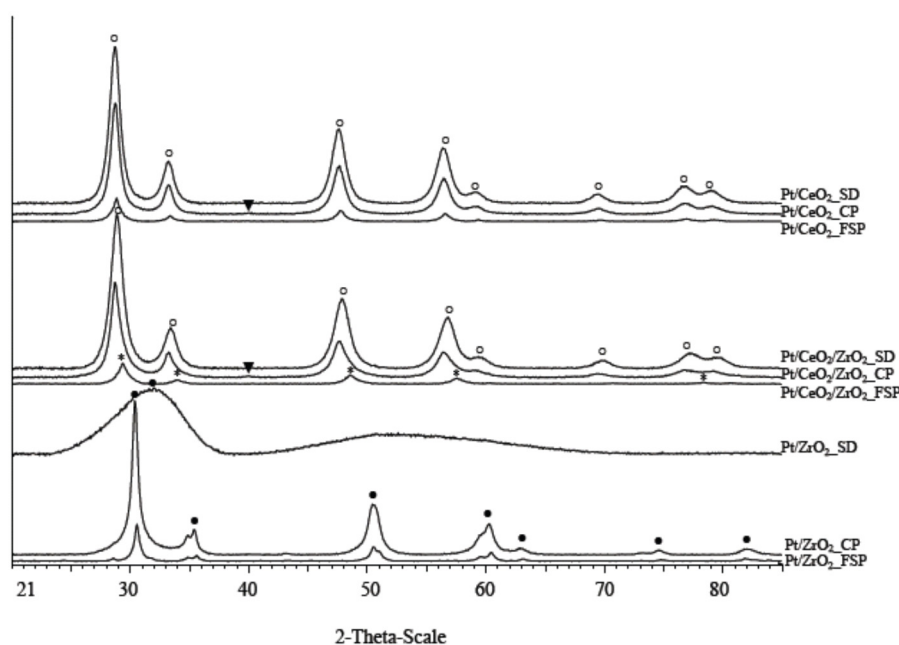


Figure 1. XRD patterns of the catalysts prepared by coprecipitation/impregnation (CP), spray drying (SD), and flame spray pyrolysis (FSP): (○) CeO_2 , (●) ZrO_2 , (*) $\text{Ce}_x\text{Zr}_{1-x}\text{O}_2$, (▼) PtO_2 .

Previous studies show the temperature at which zirconia is expected to become crystalline varies. Liang et al. [26] reported crystalline zirconia after treatment at $400\text{ }^\circ\text{C}$, while Ksapabutr et al. [27] and

Rezaei et al. [28] increased the calcination temperature to 500 and 600 °C, respectively. Devassy and Halligudi [29] detected crystalline ZrO₂ after calcination at 350 °C, but found also that the temperature had to be increased to 450 °C to obtain a crystalline phase after adding the active metal. The findings of Devassy and Halligudi partly support the results in this study, since a calcination temperature of 350 °C was enough to crystallize the support in Pt/ZrO₂_CP before the Pt impregnation, while the Pt/ZrO₂_SD may need a higher temperature. Pt/ZrO₂_FSP is exposed to higher temperatures in the flame and should therefore be expected to be crystalline. In Pt/CeO₂/ZrO₂_CP and Pt/CeO₂/ZrO₂_SD, zirconia is not found. The shift of the ceria peaks to higher 2θ values when adding zirconia to the support indicates that some of the Ce⁴⁺ are substituted by Zr⁴⁺ in the lattice [30], but also here it is possible that zirconia is present as an amorphous phase. Pt phases are only visible in the coprecipitated Pt/CeO₂ and Pt/CeO₂/ZrO₂. This is probably because the platinum particle size in the spray-dried and flame-synthesized catalysts are below the XRD detection limit.

The surface area and Pt dispersion of the catalysts are listed in Table 1. The catalysts prepared by flame spray pyrolysis have the highest surface area for all compositions and highest Pt dispersion for Pt/CeO₂ and Pt/ZrO₂. This is not surprising, since flame spray pyrolysis is known for giving high surface area materials with a good metal dispersion. Spray drying produced Pt/CeO₂ and Pt/ZrO₂ with the lowest surface area and dispersion, which is more unexpected. However, one obvious difference between FSP and SD is the lower temperature used for spray drying, which could significantly affect the catalyst properties. In addition, spray drying often results in a droplet–particle ratio of 1:1, whereas flame spray pyrolysis gives numerous nanoparticles formed from each droplet [31]. The spray-dried Pt/CeO₂/ZrO₂, on the other hand, obtained better platinum dispersion than the other Pt/CeO₂/ZrO₂ catalysts, and the surface area is also quite high. Hydrogen spillover from Pt to the support and partial reduction of the support may affect the measured hydrogen consumption and hence the measured platinum dispersion. This may not affect catalysts equally, since the reducibility of ceria and zirconia may vary between different supports and different preparation methods.

Table 1. Specific surface area, Pt dispersion, and crystallite sizes of the catalysts.

Catalyst	S _{BET} (m ² /g)	D _{Pt} (-)	D _{support} ^a (nm)	D _{Pt} ^b (nm)
Pt/CeO ₂ _CP	127	0.49	8	2.2
Pt/CeO ₂ _SD	106	0.24	8	4.6
Pt/CeO ₂ _FSP	201	0.64	10	1.7
Pt/CeO ₂ /ZrO ₂ _CP	104	0.15	7 ^c	7.3
Pt/CeO ₂ /ZrO ₂ _SD	142	0.43	6 ^c	2.6
Pt/CeO ₂ /ZrO ₂ _FSP	150	0.3	8	3.7
Pt/ZrO ₂ _CP	70	0.03	10	36.7
Pt/ZrO ₂ _SD	2	0	-	-
Pt/ZrO ₂ _FSP	118	0.14	13	7.9

^a Calculated from XRD spectra by using the Scherrer equation, ^b assuming d (nm) = 1.1/D, ^c d_{CeO₂}.

Table 1 shows that the support particle sizes of the coprecipitated and the spray-dried catalysts are similar, while flame spray pyrolysis produced slightly larger support particles. This somewhat contradicts the surface area results, since a large surface area often correlates with small particles. However, this may indicate a larger extent of agglomeration of the primary crystallites in the coprecipitated and spray-dried samples. The Pt particles are generally the smallest for the catalysts prepared by flame spray pyrolysis, but this is in principle the same as the Pt dispersion results. It was not possible to calculate the Pt particle size for Pt/ZrO₂_SD, since no hydrogen uptake was observed during the chemisorption experiment.

It is also observed that for coprecipitation and flame spray pyrolysis both the surface area and the Pt dispersion decrease with increasing zirconia content. Concerning the spray-dried catalysts, Pt/CeO₂/ZrO₂ has the highest surface area and platinum dispersion. Results reported by others show the varying influence of the ceria content, and different preparation procedures to obtain different compositions have been used in some cases [10,32–38]. The preparation method is a factor that affects

the structural properties, but definite conclusions on the correlation of different preparation methods and characterization results are difficult to find.

The TPR profiles are shown in Figure 2. Comparison of the Pt/CeO₂ catalysts shows that the reduction temperature peaks of the coprecipitated and spray-dried Pt/CeO₂ are in the same range, 100–200 °C. There are also traces of reduction of Pt/CeO₂_FSP in this temperature interval, but the main reduction lies in a much higher temperature range (350–550 °C). The amount of hydrogen consumed is highest for Pt/CeO₂_CP and quite similar for the other two. Similar trends are observed for the Pt/CeO₂/ZrO₂ samples, but the Pt/ZrO₂ samples are different. Pt/ZrO₂_CP is almost not reduced at all and Pt/ZrO₂_SD has the highest hydrogen consumption, with significantly higher reduction temperatures. To compare the coprecipitated samples, Pt/CeO₂_CP and Pt/CeO₂/ZrO₂_CP are quite similar, while Pt/ZrO₂_CP is reduced at higher temperatures (~617 °C) with substantially lower hydrogen consumption. This is also reported by others [33,39], but the most common result in the literature appears to be higher hydrogen consumption for Pt/CeO₂/ZrO₂ relative to the other two [37,40]. The reduction temperature is higher for Pt/ZrO₂_SD also for the spray-dried samples, but a lot more hydrogen is consumed in this case. The high hydrogen consumption is possibly explained by the reduction of nitrate residues, since Pt/ZrO₂_SD did not crystallize during calcination. It could also be that the oxygen present in the amorphous structure is, due to weaker bonds, more easily reacted. The spray-dried samples are all reduced in two steps. The catalysts prepared by flame spray pyrolysis are quite similar to each other in terms of reduction temperature (400–450 °C) and hydrogen consumption. Pt/CeO₂_FSP and Pt/CeO₂/ZrO₂_FSP show in addition minor peaks before 200 °C, which is absent in Pt/ZrO₂. A possible explanation as to why the spray-dried and flame-synthesized catalysts have more reduction peaks than the coprecipitated catalysts could be differences in Pt distribution and hence the availability of Pt. The platinum particles might be more distributed inside the crystal lattice for the first two methods, as opposed to the last one where Pt is impregnated on the surface. The Pt particles at the surface will probably be reduced first, and then the Pt particles in the bulk. There could also be differences in the oxidation state of Pt, and the number of reduction peaks might depend on how the support is reduced.

2.2. Activity Measurements

Figure 3a shows the CO conversion as a function of reaction temperature and Figure 3b shows the tendencies towards deactivation for all catalysts as obtained at 300/310 °C. Pt/CeO₂/ZrO₂_SD shows the highest initial CO conversion, but deactivates significantly at 300 °C. Pt/CeO₂_CP and Pt/CeO₂/ZrO₂_CP are also slightly better than the other catalysts, and they are quite similar concerning both activity and initial stability. The catalysts prepared by flame spray pyrolysis have in general the lowest activity. Based on the S_{BET} and Pt dispersion results, this was unexpected but consistent with the higher reduction temperature and a small amount of reduced Pt obtained in TPR. The stability is relatively good, however, indicating that FSP is a promising preparation method. Catalysts prepared by FSP are exposed to very high temperatures during preparation and are thereby expected to be more resistant to sintering than coprecipitated and spray-dried catalysts. This may support its good stability, since deactivation possibly occurs due to loss of metal surface area [7]. Disregarding the FSP catalysts, the ranking based on catalyst activity is closely related to the specific surface area. A correlation between high platinum dispersion and high catalytic activity when comparing the samples within the preparation methods is also present. Considering all the samples, there is no clear trend and hence the preparation method is an important factor.

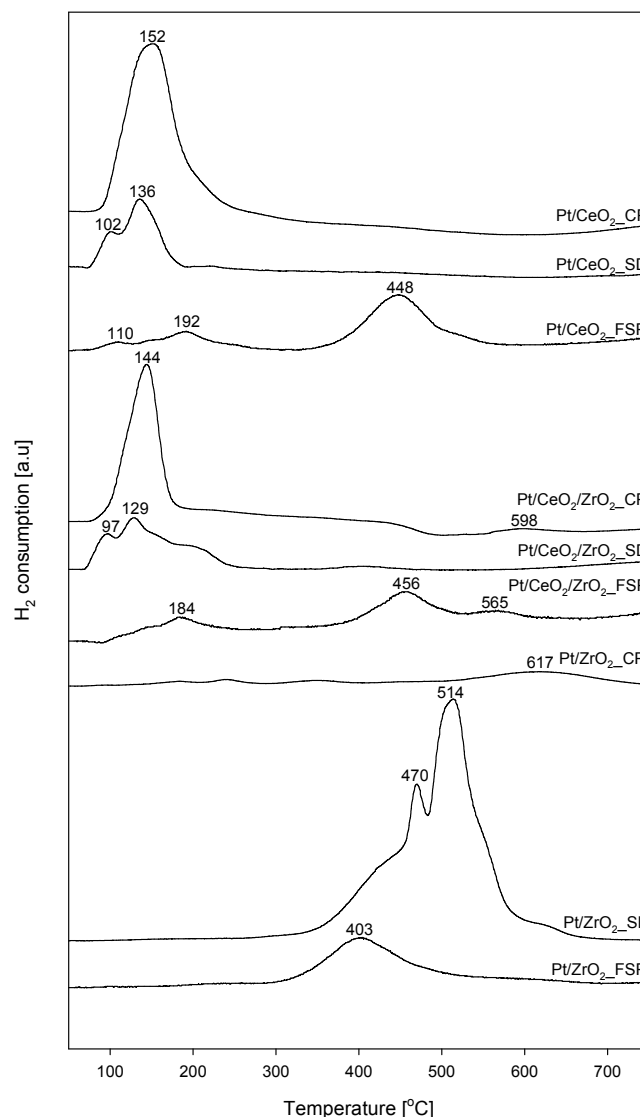


Figure 2. TPR profiles for all catalysts. Reduction in 7% H₂/Ar using a heating rate of 10 °C/min.

The crystallite size of the support also seems to be essential. With the exception of Pt/CeO₂_FSP, the smaller the support particles, the higher the activity. The specific surface area and Pt dispersion are in general expected to reflect the support particle size, but as discussed in Section 2.1, the Pt dispersion results are possibly affected by hydrogen spillover. By using the Weisz–Prater criterion it is verified that the reaction is not diffusion limited. Pt/ZrO₂_SD shows the lowest CO conversion. This was expected due to the low surface area and Pt dispersion, and the high reduction temperature. According to Tabakova et al. [41], the catalytic activity may also depend on the crystallinity of the catalyst, and the fact that Pt/ZrO₂_SD shows an amorphous phase could thereby be another contribution to the low activity. Pt/ZrO₂ is in general the less active catalyst for all preparation methods. This is related to the fact that the abovementioned properties also are quite poor for Pt/ZrO₂_CP and Pt/ZrO₂_FSP.

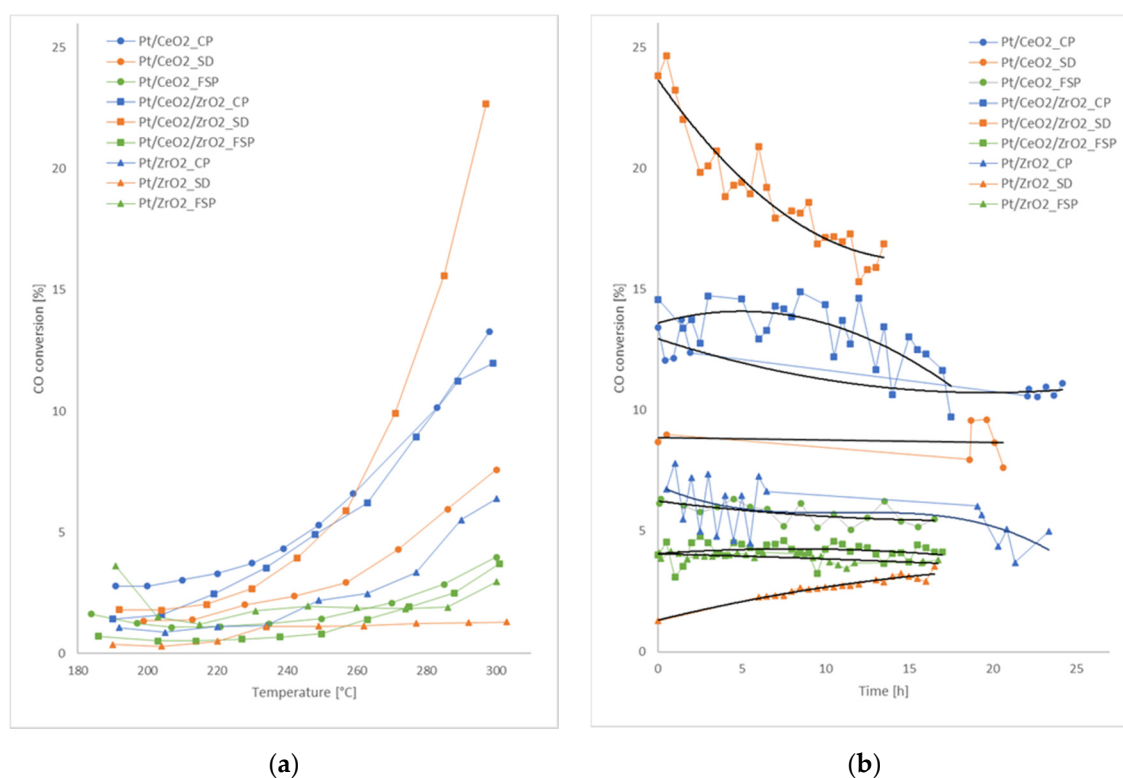


Figure 3. WGS activity as a function of (a) temperature and (b) time on stream at 300(310) °C. CP = coprecipitation/impregnation, SD = spray drying, FSP = flame spray pyrolysis.

3. Materials and Methods

3.1. Catalyst Preparation

Pt/CeO₂, Pt/ZrO₂, and Pt/CeO₂/ZrO₂ were prepared by coprecipitation/impregnation (CP), spray drying (SD), and flame spray pyrolysis (FSP) to 70/30 mol % composition of the mixed ceria/zirconia support and 2 wt % Pt loading for all catalysts.

In coprecipitation, a total amount of 0.115 mol precursors (cerium (III) nitrate hexahydrate, zirconyl (IV) nitrate hydrate (≥99.5%, Acros Organics, Geel, Belgium) were dissolved in 450 mL of a 40% ethylene glycol solution (≥99.5%, Fluka, Steinheim; Germany) in deionized water. Then, 0.99 mol urea (≥99.5%, Merck, Darmstadt, Germany) was added under stirring. The solution was placed in an oil bath (100 °C) for 16 h and then rapidly cooled in cold water. The suspension was filtered and washed 4 times with 300 mL deionized water (45 °C), and the resulting precipitate was dried (100 °C, 16 h) and calcined in a muffle furnace for 30 min at 350 °C (heating up: 2 °C/min; cooling down: ca. 2 °C/min). The calcined supports were impregnated with Pt (tetraammineplatinum (II) nitrate (99.995%, Aldrich, Steinheim, Germany)) by incipient wetness. The impregnated samples were dried and calcined in the same way as described above. Further details on the preparation method have been published elsewhere [42,43].

For spray drying, nitrate precursors (cerium (III) nitrate hexahydrate, zirconyl (IV) nitrate hydrate (≥99.5%, Acros Organics, Geel, Belgium), tetraammineplatinum (II) nitrate (99.995% (Aldrich, Steinheim, Germany) were dissolved in deionized water to give a total concentration of 10 wt %. Using a Lab-Plant SD-06 Laboratory-Scale Spray Dryer, the nitrate solution was pumped through a jet nozzle (d = 0.5 mm) and sprayed into a heated chamber. Compressed air induces droplet formation, and an outer air stream with a variable temperature separates the droplets from the nozzle and dries the material. The product flows in a continuous spiral through a cyclone and into a collection bottle. The pump rate was ~120 mL/h, the inlet temperature 165 °C, and the air flow 4.3 m/s. The samples were

calcined in a muffle furnace for 30 min at 350 °C (heating up: 2 °C/min; cooling down: ca. 2 °C/min). The Pt/ZrO₂ was calcined at 650 °C for 30 min (heating up: 2 °C/min; cooling down: ca. 2 °C/min). The principle of spray drying together with a picture of the laboratory unit is shown on Figures S4 and S5 in Supplementary.

Flame spray pyrolysis was performed in a laboratory-scale flame spray unit. Appropriate amounts of precursors (cerium (III) 2-ethylhexanoate (49% in 2-ethylhexanoic acid), platinum (II) acetylacetonate (97%), and zirconium (IV) n-propoxide (70% w/w in n-propanol, (Alfa Aesar, Karlsruhe, Germany) were dissolved in toluene (>99.7%, Riedel-de Haën, Seelze, Germany) and the solution was sprayed into a hydrogen flame at 100 mL/h by a syringe pump (IVAC P700, Cardinal Health, 1180 Rolle, Switzerland). Hydrogen was supplied at 3.1 L/min. The liquid was dispersed by 9 L/min oxygen. The product particles were collected by a glass fiber filter (Advantec GC50, Cole-Parmer, Vernon Hills, IL, USA) with the aid of a vacuum pump (PIAB M50, Hongham, MA 02043, USA). Further details on the setup are reported elsewhere [44,45] and a picture of the setup and the principle of particle formation is shown in Figures S2 and S3 in Supplementary.

3.2. Characterization

X-ray diffraction analysis of the catalysts was performed on a Bruker AXS D8 Focus diffractometer using CuK_α radiation ($\lambda = 1.54\text{\AA}$) (76187 Karlsruhe, Germany). The XRD patterns were compared with standards in a database to identify the phases and the crystallite sizes were calculated by using the Scherrer equation [46].

The specific surface area (S_{BET}) of the catalysts was determined by N₂ adsorption at −196 °C using a COULTER SA 3100 instrument. The specific surface area was calculated by the Brunauer–Emmet–Teller (BET) equation in the relative pressure interval of 0.05–0.20. Prior to the measurements, the samples were outgassed at 150 °C for 2 h.

The Pt dispersion was determined by H₂ chemisorption, using a Micromeritics ASAP 2010 (Norcross, GA, USA) instrument. An amount of 0.2 g catalyst was loaded into a quartz reactor and held in place by quartz wool. Prior to the chemisorption measurement, the samples were reduced in H₂ flow while heating at 10 °C/min up to 300 °C. The samples were then evacuated in He flow at 300 °C for 1 h before cooling down to 35 °C, at which the analysis was performed. In order to distinguish between chemisorbed and physisorbed hydrogen, two adsorption isotherms were measured.

Temperature-programmed reduction (TPR) experiments were performed using a Quantachrome CHEMBET 3000 (Boynton Beach, FL, USA) instrument, where the effluent gas is analyzed by a thermal conductivity detector (TCD). An amount of 0.15 g catalyst was loaded into a quartz reactor and quartz wool was used to keep it in place. The samples were outgassed in Ar flow at 300 °C for 1 h prior to the measurements, and after cooling down to ambient temperature, the samples were heated in 7% H₂/Ar (60 mL/min) at 10 °C/min up to 800 °C.

3.3. Activity Measurements

WGS activity measurements were carried out in a fixed-bed reactor using 0.10 g catalyst diluted with SiC (50/50 vol%). The catalysts were prereduced at 220 °C for three hours in 20% hydrogen in nitrogen (5% H₂ in N₂ for the FSP catalysts) at a total gas flow of 100 N mL/min. A 1:1:1 mixture of N₂, CO, and steam was fed at 150 N mL/min total flow during reaction experiments, and the pressure was close to ambient. Measurements were performed in the temperature interval 190–300 °C, and the initial catalyst deactivation was studied at 300 °C (310 °C for the FSP catalysts) by doing repeated measurements for 15–20 h. The dry product gas (H₂, CO, CO₂, N₂) was analyzed using an Agilent 3000 Micro GC (Santa Clara, CA, USA). A flowsheet of the experimental setup is given as Figure S1 in Supplementary.

4. Conclusions

It is shown that the preparation method is of importance concerning the properties of the Pt-based catalysts, and thereby the water–gas shift activity. The spray-dried Pt/CeO₂/ZrO₂ catalyst shows the highest initial activity, but deactivates rapidly at 300 °C, and levels out at similar activity as the coprecipitated Pt/CeO₂ and Pt/CeO₂/ZrO₂ within a few hours. The more stable Pt/CeO₂_CP could have become the most active if the stability were tested for a longer period. Flame spray pyrolysis appears to be a promising preparation method concerning the stability of the catalysts. However, the initial activity is rather poor, although this could be attributed to incomplete reduction. High activity is related to high Pt dispersion, low reduction temperature, and small support particles. The Pt dispersion is an important factor, but the measurements are complicated due to spillover when Pt is supported on reducible supports such as ceria and zirconia. A comparison of the dispersion results and the activity measurements indicate that the reducibility of the support could vary between the different preparation methods. Additionally, the support particle size is much affected by the preparation method.

Supplementary Materials: The following are available online at <http://www.mdpi.com/2073-4344/10/10/1132/s1>, Figure S1: Schematic presentation of the experimental setup used for water-gas activity testing. Figure S2: The principle of particle formation in a flame. Figure S3: The setup for flame spray pyrolysis employed at DTU. Figure S4: The principle of spray drying. Figure S5: The Lab-Plant SD-06 Laboratory spray dryer.

Author Contributions: Conceptualization: H.J.V., A.H. methodology: M.R., T.J. experimental investigation: H.B. writing—original draft preparation: H.B., writing—review and editing: A.H., H.J.V. All authors have read and agreed to the published version of the manuscript.

Funding: Financial support was provided by the Research Council of Norway through the projects 153967/420—Scientific Design and Preparation of New Catalysts and Supports and 158516/S10 (NANOMAT) and through a travel grant from the Strategic Area Materials at NTNU.

Conflicts of Interest: The authors declare no conflict of interest.

References

1. Ratnasamy, C.; Wagner, J.P. Water Gas Shift Catalysis. *Catal. Rev.* **2009**, *51*, 325–440. [[CrossRef](#)]
2. Holladay, J.D.; Wang, Y.; Jones, E. Review of Developments in Portable Hydrogen Production Using Microreactor Technology. *Chem. Rev.* **2004**, *104*, 4767–4790. [[CrossRef](#)]
3. Ladebeck, J.R.; Wagner, J.P. *Handbook of Fuel Cells—Fundamentals, Technology and Applications, Vol. 3: Fuel Cell Technology and Applications*; Vielstich, W., Gasteiger, H.A., Lamm, A., Eds.; Wiley and Sons: New York, NY, USA, 2003; pp. 190–201.
4. Palma, V.; Ruocco, C.; Cortese, M.; Renda, S.; Meloni, E.; Festa, G.; Martino, M. Platinum Based Catalysts in the Water Gas Shift Reaction: Recent Advances. *Metals* **2020**, *10*, 866. [[CrossRef](#)]
5. Bunluesin, T.; Gorte, R.; Graham, G. Studies of the water-gas-shift reaction on ceria-supported Pt, Pd, and Rh: Implications for oxygen-storage properties. *Appl. Catal. B Environ.* **1998**, *15*, 107–114. [[CrossRef](#)]
6. Zalc, J.; Sokolovskii, V.; Löffler, D. Are Noble Metal-Based Water–Gas Shift Catalysts Practical for Automotive Fuel Processing? *J. Catal.* **2002**, *206*, 169–171. [[CrossRef](#)]
7. Wang, X.; Gorte, R.J.; Wagner, J. Deactivation Mechanisms for Pd/Ceria during the Water–Gas-Shift Reaction. *J. Catal.* **2002**, *212*, 225–230. [[CrossRef](#)]
8. Kašpar, J.; Fornasiero, P. Nanostructured materials for advanced automotive de-pollution catalysts. *J. Solid State Chem.* **2003**, *171*, 19–29. [[CrossRef](#)]
9. Ozawa, M. Role of cerium–zirconium mixed oxides as catalysts for car pollution: A short review. *J. Alloy. Compd.* **1998**, *275–277*, 886–890. [[CrossRef](#)]
10. Ricote, S.; Jacobs, G.; Milling, M.; Ji, Y.; Patterson, P.M.; Davis, B.H. Characterization and testing of binary mixed oxides of ceria and zirconia promoted with Pt. *Appl. Catal. A Gen.* **2006**, *303*, 35–47. [[CrossRef](#)]
11. Letichevsky, S.; Tellez, C.A.; De Avillez, R.R.; Da Silva, M.I.P.; Fraga, M.A.; Appel, L.G. Obtaining CeO₂–ZrO₂ mixed oxides by coprecipitation: Role of preparation conditions. *Appl. Catal. B Environ.* **2005**, *58*, 203–210. [[CrossRef](#)]
12. Mohamed, M.M.; Salama, T.; Othman, A.; El-Shobaky, G. Low temperature water-gas shift reaction on cerium containing mordenites prepared by different methods. *Appl. Catal. A Gen.* **2005**, *279*, 23–33. [[CrossRef](#)]

13. Tabakova, T.; Boccuzzi, F.; Manzoli, M.; Sobczak, J.W.; Idakiev, V.; Andreeva, D. Effect of synthesis procedure on the low-temperature WGS activity of Au/ceria catalysts. *Appl. Catal. B Environ.* **2004**, *49*, 73–81. [[CrossRef](#)]
14. Zerva, C.; Philippopoulos, C. Ceria catalysts for water gas shift reaction: Influence of preparation method on their activity. *Appl. Catal. B Environ.* **2006**, *67*, 105–112. [[CrossRef](#)]
15. Jensen, J.R. Flame Synthesis of Composite Oxides for Catalytic Applications. Ph.D. Thesis, Technical University of Denmark, Lyngby, Denmark, 2001.
16. Hansen, J.P.; Jensen, J.R.; Livbjerg, H.; Johannessen, T. Synthesis of ZnO particles in a quench-cooled flame reactor. *AIChE J.* **2001**, *47*, 2413–2418. [[CrossRef](#)]
17. Johannessen, T.; Jensen, J.; Mosleh, M.; Johansen, J.; Quaade, U.; Livbjerg, H. Flame Synthesis of Nanoparticles: Applications in Catalysis and Product/Process Engineering. *Chem. Eng. Res. Des.* **2004**, *82*, 1444–1452. [[CrossRef](#)]
18. Meland, H.; Johannessen, T.; Arstad, B.; Venvik, H.J.; Rønning, M.; Holmén, A. Preparation of low temperature water-gas shift catalysts by flame spray pyrolysis. *Stud. Surf. Sci. Catal.* **2006**, *162*, 985–992.
19. Lee, D.; Ha, G.; Kim, B.K. Synthesis of Cu-Al₂O₃ nano composite powder. *Scr. Mater.* **2001**, *44*, 2137–2140. [[CrossRef](#)]
20. Robertz, B.; Boschini, F.; Rulmont, A.; Cloots, R.; Van Driessche, I.; Hoste, S.; Lecomte-Beckers, J. Preparation of BaZrO₃ powders by a spray-drying process. *J. Mater. Res.* **2003**, *18*, 1325–1332. [[CrossRef](#)]
21. Nelson, N.C.; Szanyi, J. Heterolytic Hydrogen Activation: Understanding Support Effects in Water–Gas Shift, Hydrodeoxygenation, and CO Oxidation Catalysis. *ACS Catal.* **2020**, *10*, 5663–5671. [[CrossRef](#)]
22. Ginés, M.; Amadeo, N.; Laborde, M.; Apesteguía, C. Activity and structure-sensitivity of the water-gas shift reaction over Cu, Zn, Al mixed oxide catalysts. *Appl. Catal. A Gen.* **1995**, *131*, 283–296. [[CrossRef](#)]
23. Saito, M.; Wu, J.; Tomoda, K.; Takahara, I.; Murata, K. Effects of ZnO Contained in Supported Cu-Based Catalysts on Their Activities for Several Reactions. *Catal. Lett.* **2002**, *83*, 1–4. [[CrossRef](#)]
24. Saito, M.; Tomoda, K.; Takahara, I.; Murata, K.; Inaba, M. Effects of Pretreatments of Cu/ZnO-Based Catalysts on Their Activities for the Water–Gas Shift Reaction. *Catal. Lett.* **2003**, *89*, 11–13. [[CrossRef](#)]
25. Choung, S.Y.; Ferrandon, M.; Krause, T. Pt-Re bimetallic supported on CeO₂-ZrO₂ mixed oxides as water–gas shift catalysts. *Catal. Today* **2005**, *99*, 257–262. [[CrossRef](#)]
26. Liang, L.; Xu, Y.; Hou, X.; Wu, N.; Sun, Y.; Li, Z.; Wu, Z. Small-angle X-ray scattering study on the microstructure evolution of zirconia nanoparticles during calcination. *J. Solid State Chem.* **2006**, *179*, 959–967. [[CrossRef](#)]
27. Ksapabutr, B.; Gulari, E.; Wongkasemjit, S. Preparation of zirconia powders by sol–gel route of sodium glycozirconate complex. *Powder Technol.* **2004**, *148*, 11–14. [[CrossRef](#)]
28. Rezaei, M.; Alavi, S.M.; Sahebdehfar, S.; Yan, Z.-F. Tetragonal nanocrystalline zirconia powder with high surface area and mesoporous structure. *Powder Technol.* **2006**, *168*, 59–63. [[CrossRef](#)]
29. Devassy, B.M.; Halligudi, S. Effect of calcination temperature on the catalytic activity of zirconia-supported heteropoly acids. *J. Mol. Catal. A Chem.* **2006**, *253*, 8–15. [[CrossRef](#)]
30. Fan, J.; Wu, X.; Ran, R.; Weng, D. Influence of the oxidative/reductive treatments on the activity of Pt/Ce_{0.67}Zr_{0.33}O₂ catalyst. *Appl. Surf. Sci.* **2005**, *245*, 162–171. [[CrossRef](#)]
31. Seo, D.J.; Park, S.B. Preparation of ferrite nanoparticles by flame-assisted spray pyrolysis. In Proceedings of the European Aerosol Conference 2003, Madrid, Spain, 31 August–5 September 2003.
32. Chenu, E.; Jacobs, G.; Crawford, A.C.; Keogh, R.A.; Patterson, P.M.; Sparks, D.E.; Davis, B.H. Water-gas shift: An examination of Pt promoted MgO and tetragonal and monoclinic ZrO₂ by in situ drifts. *Appl. Catal. B Environ.* **2005**, *59*, 45–56. [[CrossRef](#)]
33. Perez-Hernandez, R.; Aguilar, F.; Gómez-Cortés, A.; Diaz, G. NO reduction with CH₄ or CO on Pt/ZrO₂-CeO₂ catalysts. *Catal. Today* **2005**, *107–108*, 175–180. [[CrossRef](#)]
34. Azzam, K.; Babich, I.; Seshan, K.; Lefferts, L. Bifunctional catalysts for single-stage water–gas shift reaction in fuel cell applications. Part 1. Effect of the support on the reaction sequence. *J. Catal.* **2007**, *251*, 153–162. [[CrossRef](#)]
35. Panagiotopoulou, P.; Papavasiliou, J.; Avgouropoulos, G.; Ioannides, T.; Konarides, D.I. Water–gas shift activity of doped Pt/CeO₂ catalysts. *Chem. Eng. J.* **2007**, *134*, 16–22. [[CrossRef](#)]
36. Querino, P.S.; Bispo, J.R.C.; Rangel, M. The effect of cerium on the properties of Pt/ZrO₂ catalysts in the WGS. *Catal. Today* **2005**, *107–108*, 920–925. [[CrossRef](#)]

37. Passos, F.B.; De Oliveira, E.R.; Mattos, L.V.; Noronha, F.B. Partial oxidation of methane to synthesis gas on Pt/Ce_xZr_{1-x}O₂ catalysts: The effect of the support reducibility and of the metal dispersion on the stability of the catalysts. *Catal. Today* **2005**, *101*, 23–30. [[CrossRef](#)]
38. Mikulová, J.; Rossignol, S.; Barbier, J.; Duprez, D., Jr.; Kappenstein, C. Characterizations of platinum catalysts supported on Ce, Zr, Pr-oxides and formation of carbonate species in catalytic wet air oxidation of acetic acid. *Catal. Today* **2007**, *124*, 185–190. [[CrossRef](#)]
39. Ayastuy, J.; González-Marcos, M.; Gil-Rodríguez, A.; González-Velasco, J.; Gutiérrez-Ortiz, M.A. Selective CO oxidation over Ce_xZr_{1-x}O₂-supported Pt catalysts. *Catal. Today* **2006**, *116*, 391–399. [[CrossRef](#)]
40. Mattos, L.V.; Noronha, F.B. Partial oxidation of ethanol on supported Pt catalysts. *J. Power Sources* **2005**, *145*, 10–15. [[CrossRef](#)]
41. Tabakova, T.; Idakiev, V.; Andreeva, D.; Mitov, I. Influence of the microscopic properties of the support on the catalytic activity of Au/ZnO, Au/ZrO₂, Au/Fe₂O₃, Au/Fe₂O₃-ZnO, Au/Fe₂O₃-ZrO₂ catalysts for the WGS reaction. *Appl. Catal. A Gen.* **2000**, *202*, 91–97. [[CrossRef](#)]
42. Huber, F.; Venvik, H.J.; Ronning, M.; Walmsley, J.C.; Holmen, A. Preparation and characterization of nanocrystalline, high-surface area Cu, Ce, Zr mixed oxide catalysts from homogeneous co-precipitation. *Chem. Eng. J.* **2008**, *137*, 686–702. [[CrossRef](#)]
43. Huber, F.; Yu, Z.; Walmsley, J.C.; Chen, D.; Venvik, H.J.; Holmen, A. Nanocrystalline Cu-Ce-Zr mixed oxide catalysts for water-gas shift: Carbon nanofibers as dispersing agent for the mixed oxide particles. *Appl. Catal. B Environ.* **2007**, *71*, 7–15. [[CrossRef](#)]
44. Johannessen, T.; Johansen, J.; Mosleh, M.; Thybo, S.; Quaade, U.; Jensen, J.R.; Livbjerg, H. Application of nano-particles produced by flame aerosol methods. In Proceedings of the International Congress for Particle Technology (PARTEC 2004), Nuremberg, Germany, 16–18 March 2004.
45. Thybo, S.; Jensen, S.; Johansen, J.; Johannessen, T.; Hansen, O.; Quaade, U.J. Flame spray deposition of porous catalysts on surfaces and in microsystems. *J. Catal.* **2004**, *223*, 271–277. [[CrossRef](#)]
46. Niemantsverdriet, J.W. X-ray Diffraction. In *Spectroscopy in Catalysis, An Introduction*; Wiley-VCH: Weinheim, Germany, 2000; pp. 138–145.



© 2020 by the authors. Licensee MDPI, Basel, Switzerland. This article is an open access article distributed under the terms and conditions of the Creative Commons Attribution (CC BY) license (<http://creativecommons.org/licenses/by/4.0/>).